# DISCIPLINARY SUB-PROCESSES TO ASSESS LOW-SPEED PERFORMANCE AND NOISE CHARACTERISTICS WITHIN AN AIRCRAFT DESIGN ENVIRONMENT

B. Fröhler[1)], C. Hesse[1)], G. Atanasov[1)], P. Wassink[1)]
[1)] DLR Institute of System Architectures in Aeronautics, Hamburg

**Abstract**

The overall aircraft assessment is based on a wide range of disciplinary methodologies. In addition, a consistent aircraft design must be provided for the beginning of the aircraft design process. For this purpose, the DLR in-house conceptual aircraft design tool *openAD* has been developed for initialization and subsequent synthesis of results with higher fidelity. Within the aircraft design process, three disciplinary methods are introduced to improve the quality and accuracy of the performed design studies. These methods include engine performance, low speed performance and acoustics characteristics of an aircraft, which allows the predictions of the aircraft performance and noise level during the take-off and landing phase.

The engine performance calculation is based on a thermodynamic cycle model and is an extension in *openAD*. Subsequently, the aircraft and engine performance are fed into the low speed performance tool *LSperfo*, which estimates the take-off and landing trajectory including the thrust requirements, flight path and aerodynamic forces. The aircraft and engine data are further passed to a noise tool, which predicts the aircraft model noise emission at relevant aircraft certification points.

To demonstrate the result validity of the aircraft design environment and its disciplinary tools, a DLR interpretation of a turboprop engine aircraft (ATR 72 similar) is used. Since the tools are based on simple physical models, a proper calibration on appropriate reference aircraft needs be ensured for most overall aircraft design studies. Nevertheless, the results show a good estimation for take-off and landing field length as well as the noise level of the reference cases provided in this paper.

**Keywords**

Conceptual aircraft design, multidisciplinary design and analysis, low speed performance, Aircraft noise prediction,

## 1 INTRODUCTION

A competitive and innovative aircraft design is essential to achieve the ambitious goals of the Flightpath 2050 [1]. The assessment of an aircraft design, even at conceptual level, is of particular challenge due to high degree of interactions between the different disciplines. Using disciplinary tools in the early stage of an aircraft design, will improve the decision-making processes and consequently the vehicle performance itself.

The workflow-driven integration environment RCE [2], allows for a collaborative and distributed work between different DLR institutes and external partners. The RCE framework supports the integration and combination of software components from local or remote locations for a combined workflow. The workflows sub-processes of multidisciplinary and multi-fidelity tools communicate thought their inputs and outputs using the common language CPACS [3], [4]. CPACS is a data definition schema for air transport systems. It describes the characteristics of aircraft, including geometry data, aerodynamic polar, mass properties, propulsion system information, performance requirements and noise characteristics.

At the beginning of an aircraft design process, using different disciplinary sub-processes, a consistent reference must be made available. For this purpose, the conceptual aircraft design tool *openAD* [5] has been developed in the past years at the German Aerospace Centre (DLR). *OpenAD* is used to initialise the workflow with a minimum set of top-level aircraft requirements (TLARs) and design parameters. Subsequently, disciplinary tools are used to refine the results of *openAD* with higher fidelity methods.

This paper presents advances in the multidisciplinary aircraft design environment and expands the DLR tool environment of disciplinary sub-processes. The key objective is the development of methods to compute the engine performance, low speed performance and basic noise characteristics of an aircraft.



doi: 10.25967/530201

Previously, the DLR in-house tool *GTlab* (Gas Turbine Laboratory), developed by the DLR institute of Propulsion Technology, provided the predefined engine performance decks, which were imported into the aircraft design process [6]. However, the need to generate fast engine performance decks, with lower fidelity and with sensitivities on e.g. off-takes or geometrical parameters, emerged to be essential to run engine trade studies within an aircraft design process. Within the scope of this work, the conceptual aircraft design tool *openAD* [5] has been adapted with an analytical calculation of the engine thermodynamics cycle to export an engine performance deck, which meets the requirements of the overall aircraft design.
Currently, a low speed performance method is not available for the RCE environment. As of now, some low speed characteristics are estimated within *openAD*, however, a detailed analysis for a subsequent noise prediction is missing. Therefore, the tool *LSperfo* is developed to account for the aircraft performance during the take-off and landing phase depending on the aircraft geometry, aerodynamics and engine performance.
The simulation tool *PANAM* [7], [8] is DLR's reference noise source modelling and noise assessment capability. However, the new developed method with lower fidelity supports a fast and simple implementation into future CPACS versions. Therefore, the proposed method can be used for fast and simplified noise trade indications in very early conceptual overall aircraft design phases. With more information available about the overall aircraft, *PANAM* should be used for proper noise assessment.

The presented paper will give an overview of a general overall aircraft design process and will describe in depth the developed methods to extent the design process. Finally, based on the introduced methods, results are demonstrated for a DLR interpretation of the ATR–72 similar aircraft configuration.

## 2 OVERALL AIRCRAFT DESIGN ENVIRONMENT

To evaluate the design space and the overall aircraft characteristics, a multidisciplinary design workflow is set up in RCE. The workflow is composed of the main disciplines needed for the overall aircraft design (OAD) such as aerodynamics, structural design, propulsion systems, mission definitions and performance calculations as well as more detailed disciplines like acoustics.

The OAD process is divided into different levels of fidelity, ranging from level 0 to level 2, to ensure an appropriate effort of computational cost for each domain. L0 methods are based on semi-empirical equations to allow for a robust initial design and preliminary exploration of the design space. Within the L1 domain, methodologies are based on simplified physics and used semi-analytical or simple numerical calculations. This domain is employable for an extension of the design space or refining the results provided by the lower fidelity methods. The L2 methods are based on higher-order methods with a disciplinary representation of the design problem by a more detailed description of the geometry or underlying physics. Consequently, the computational cost will increase multiple orders of magnitude for each shift in level of fidelity.

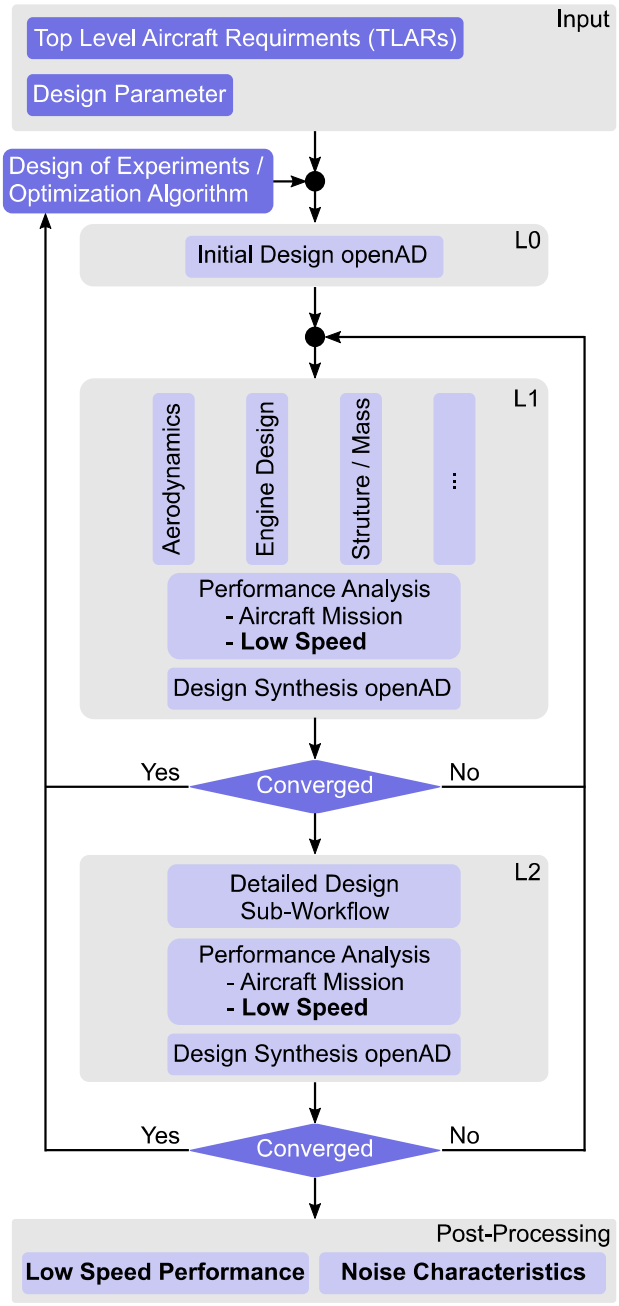


Figure 1 Flowchart of the overall aircraft design workflow [5]

Figure 1 illustrates an OAD process using different levels of fidelity and post-processing tools. First of all, the TLARs, i.e. design range, cruise altitude, Mach number, payload definition, take-off and landing field length, and the reserve mission specification need to be specified. Project specific boundary conditions of the overall aircraft model need to be specified as well, i.e. overall aircraft configuration, pre-

defined geometry of specific. The process is then initiated by the L0 tool *openAD*, which is based on well understood handbook methods, e.g. by TORENBEEK [9], [10] ROSKAM [11], RAYMAR [12], WELLS et al. [13], JENKINSON et al. [14] and is extended by in-house methods. In the frame of this work, the engine performance calculation within *openAD* was enhanced to output a complete engine deck. *OpenAD* will export the results in a CPACS format, which captures the aircraft model description in a predefined schema and thereby, serves as a consistent interface between the different tools.

The L1 domain is dedicated to the disciplinary tools, which refine the calculation of the aerodynamics, engine performance and the masses of specific airframe components. Subsequently, the DLR in-house tool AMC by Silberhorn [15] is applied to compute the aircraft performance and merge the outcome of disciplinary tools. At this stage, the low speed performance tool *LSperfo* is added for the take-off and landing performance. To synthesise the results of higher fidelity methods, the *openAD* input is updated by the L1 results. Any parameter of the aircraft model calculated by *openAD* can also be predefined in the input, which overrides the calculation of the parameter. The predefined parameter serves as a boundary condition for the overall aircraft model, affecting the final solution. The synthesized model is fed back to the disciplinary tools for a new iteration. The described L1 loop is iterated until convergence.
The L2 domain includes detailed sub-environments for in depth analysis of design studies and project specific tasks. Similarly, to the L1 domain, the L2 domain will perform a mission performance analysis and feedback the results to *openAD* for the synthesis.

Once the overall aircraft parameters re converged, post-processing tools will provide additional information to the design i.e. payload-range characteristics, direct operating cost or climate impact. The low-speed tool *LSperfo* plays an important part in the convergence of the L1 and L2 loops and is used for the post-processing routine as well. The noise calculation tool is used for post-processing only. Both tools, as well as the engine performance calculation in *openAD*, will be described more in detail in the next section.

## 3 DISCIPLINARY SUB-PROCESSES

### 3.1 Engine Performance Methodology

As mentioned in Section 1, the engine performance is calculated at a conceptual level in the overall aircraft design tool *openAD*. The model follows the engine cycle synthesis approach of BRAUENLING [16]. The modelling includes the following aspects:

- Specific heat dependency of the gas on the temperature and on the portion of fuel to air mixture.
- Polytropic compression and expansion.
- Pressure drop in the diffusor, combustion chamber, and nozzle.
- Mechanical efficiency for the power transfer from the turbine to the compressor, fan, or power shaft.
- Cooling air from the compressor for turbine stages operating at high temperatures.
- Electric and bleed air offtakes.

The computation assumes that the engine is optimized for a specified design point, defined by altitude, flight Mach number, and temperature deviation from the international standard atmosphere (ISA) model. If the design point is not specified, the design mission mid-cruise condition calculated for the overall aircraft sizing loop is assumed. The overall pressure ratio (OPR) and the turbine entry temperature (TET), as well as the bypass ratio (BPR) in case of a turbofan engine, of the design point need to be specified. If not specified by the user, *openAD* assumes empirical values depending on the engine type and power level.

The component efficiencies are determined in a top-down approach, where a target overall gas turbine efficiency is provided as an input, either specified by the user or determined empirically. The component efficiencies and pressure losses are adjusted by the program to meet the target efficiency. An ideal overall efficiency, which assumes no component losses, is calculated to serve as a crosscheck to help the user avoid unrealistic solutions.
The calculation of the design point determines the temperature and pressure at each station and as a result the specific power and thrust of the gas turbine. The model makes use of the following assumptions:

- A near-optimum jet velocity in terms of overall efficiency is assumed fixed for the design point. Simple methods for determining this velocity for turbofan and turboprop engines are taken from BRAUENLING [16].
- Turboprop gas turbines assume critical flow at the free turbine, which drives the propeller, as suggested by BRAUENLING [16].
- Turbofan gas turbines assume critical flow at the high-pressure turbine, directly after the combustion chamber, as suggested by BRAUENLING [16].

After the design point is determined, off-design points are calculated. The calculation is simplified, assuming component efficiencies identical to the design point. The pressure ratios of the turbine stages are set equal to the design point result as well. These simplifications work well for operating points with high power level and for a significant portion of the partial power spectrum. Since the aircraft sizing mostly considers the high-power level operation, such a simplification is well suited for conceptual-level studies. The most notable exceptions are descent and taxi modelling, where a slightly different approach in the engine performance calculation is taken. However, these phases are of a secondary significance for the overall model and are outside the scope of the current paper.

At this point, the size of the engine is still not determined, as the calculation is normalized with respect to power output at the design point. The following requirements are considered in *openAD* for determining the size of the engine:

- Sea-Level Static Thrust (SLST) at ISA conditions and Maximum Take-Off (MTO) rating.
- SLST at specified airport conditions and MTO rating.
- First segment climb thrust requirement at specified airport conditions (CS 25.121 (a)) and Reserve Take-Off (RTO) rating.
- Second segment climb thrust requirement at specified airport conditions (CS 25.121 (b)) and RTO rating.
- Top of Climb (TOC) thrust requirement at specified TOC conditions and Maximum Climb (MCL) rating.
- Cruise thrust requirements at initial cruise conditions and Maximum Cruise (MCR) rating.

Each gas turbine rating has a TET limit, either specified by the user or empirically determined by *openAD*.
For the initial aircraft design (L0) in the overall aircraft sizing model, shown in Figure 1, the requirements are derived by *openAD*. For the design synthesis (L1 in Figure 1), the low speed thrust requirements are derived by the Low Speed Performance Tool (see Section 3.2), whereas the high-speed requirements are derived by AMC (see Section 2), and used in the *openAD* input, thus overwriting the L0 calculation.

The calculated requirements are used to determine the size of the engine, in terms of mass flow rate, as well as power and thrust output at the design point.
The sized engine model is used in the post-processing routine of *openAD* to generate engine decks in CPACS format including any parameters needed by the L1-stage tools of the overall aircraft sizing model shown in Figure 1.

## 3.2 Low Speed Performance Tool

The low speed performance tool *LSperfo* is able to perform take-off and landing trajectory performance calculations by stepwise solving the 2D equation of motion (Equation (1) and (2)) at different operating condition i.e. all engine operating (AEO), one engine inoperative (OEI) or rejected take-off (RTO). The coordinate system is based on Figure 2.

(1) $x_a$: $\frac{W}{g}\, a = T \cdot \cos(\alpha + \iota_T) - D - W \cdot \sin(\gamma)$

(2) $z_a$: $0 = T \cdot \sin(\alpha + \iota_T) + L - W \cdot \cos(\gamma)$

The tool is python based and partitioned in pre-processing, solver and post-processing. The pre-processing reads the CPACS input and interprets the aircraft specific data, which are needed for the solver. The input needs to include a necessary set of parameters such as take-off mass, maximum lift coefficient and number of engines. Additionally, the engine performance deck and aerodynamic performance with and without control surface deflection are necessary and can be specified for each flight-path segment. The different flight-path segments can be adjusted within the mission definitions with the thrust settings or a maximum flight path angle. Tool specific settings are also necessary, such as the time step, airport parameter, i.e. elevation and runway gradient, and mission specific data. The tool specific settings were analysis and results showed, a time step of dt = 0.1 or lower should be used to avoid high fluctuations of the results. The position at which the aircraft retracts the control surfaces, is recommended to be at a $c_L$ = 1.0 and with a retraction time of minimum

(3) $$t_{Retaction} \geq \frac{dt}{\text{Retraction Step}} \geq 5\ \text{sec}$$

to assure a technically feasible retraction process.

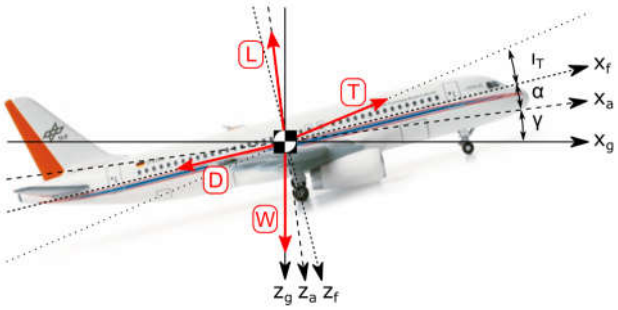


Figure 2 Aircraft coordinate system

The solver operates in four modes, the default mode 0 where the AEO case for both take-off and landing is analysed. Mode 1 calculates the balanced field-length using the take-off configurations AEO, OEI and RTO. The mode 2 and mode 3 calculate take-off and landing sensitivities, respectively, for the AEO case with varying the airport elevation and the starting aircraft mass.

The post-processing part writes a CPACS output file, including the corresponding trajectories, and additional results for further post-processing applications.

### 3.2.1 Take – Off Performance

The take-off path, illustrated in Figure 3, is divided into five segments and additionally, a climb segment, as described in the Airbus manual [17]. For each segment the 2D equation of motion is solved with a constant time step, but changed for different aircraft configurations and settings.

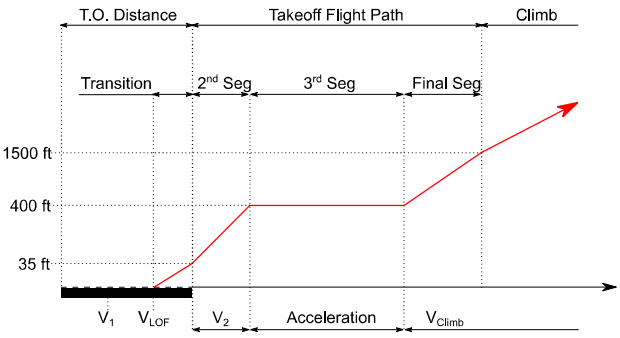


Figure 3 Take-off path and definition of Segments [17]

The AEO case represents an ordinary take-off procedure, starting with the take-off distance at the airport, continuing with the take-off flight path and climb segment.
During the *ground roll* segment, the aerodynamic performance is interpolated from the corresponding aerodynamic performance map with control surfaces in take-off arrangement and landing gear extracted. As soon as the lift-off speed,

(4) $$v_{LOF} = v_S \cdot 1.15,$$

with $v_S$ as the stall speed, is reached, the aircraft model is assumed to be airborne.
The subsequent *transition* segment exhibits the same configuration as during ground roll with control surfaces in take-off configuration and extended landing gear. During this segment, the aircraft accelerates upon the take-off climb speed $v_2$, which should be higher than $v_{2_{min}}$ and must be reached at a height of 35ft above ground:

(5) $$v_{2_{min}} \geq v_S \cdot 1.13$$

With stall speed $v_s$:

(6) $$v_s = \sqrt{\frac{2}{\rho c_{L,max}} \cdot \frac{W}{S}}$$

Above 35ft, the *2nd* segment is initiated in which the landing gear is retracted and the aircraft is flying at a constant calibrated airspeed (CAS) and the *2nd* segment control surfaces configuration. The aircraft must maintain a minimum climb gradient of 2.4% or 3.0% for twin or quad engines, respectively, with n-1 engines operating. The *2nd* segment ends at an altitude of 400ft and continues with a level flight during the *3rd* segment.
The *3rd* segment is an acceleration segment and the control surfaces are retracted. The segment starts with the take-off climb speed $v_2$ and accelerates up to a prescribed climb speed. First, the aircraft accelerates up to a desired lift coefficient $c_L$, and then a stepwise retraction of the control surfaces starts. Here, between the aerodynamic performances of the *2nd* segment, with control surfaces deflected, and the clean configuration is interpolated.
The *final segment* is initiated once the climb speed is reached. A constant CAS is prescribed and the aircraft is in clean configuration. At an altitude of 1500ft, the take-off flight path is finalised and continues with the *climb* segment. To have sufficient performance data for the noise estimation, the flight path continues with the *climb* segment up to 10km.

The OEI or RTO cases follow a similar procedure as for the AEO case. At the ground roll segment, the aircraft experiences an engine failure at a given speed $v_{EF}$, in which one engine thrust is set to zero. Thus, acceleration and thrust of the aircraft is reduced, which results in a longer take-off flight path or stopping the aircraft by applying breaks. At the decision speed $v_1$, 1 second after the engine failure, the pilot has to decide to reject or complete the take-off. An increase in $v_1$ leads to a reduction in take-off distance, due to a longer acceleration phase of all engines operating. But on the other hand, an increase of $v_1$ will increase the acceleration stop distance, due to a higher aircraft speed.

Figure 4 depicts the general process to find the minimum decision speed for a given available take-off length by varying $v_1$ or finding the balanced field length by interpolating between the OEI and RTO cases.

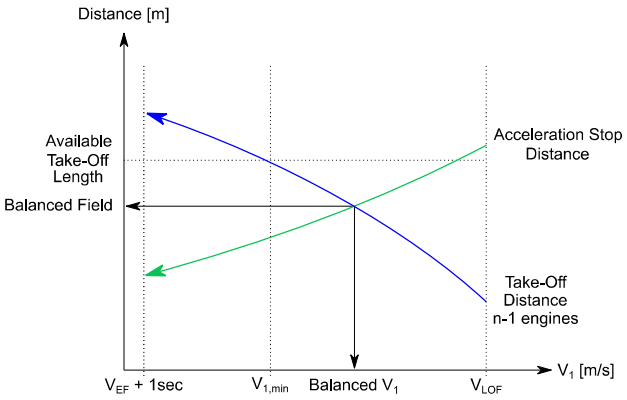


Figure 4 Influence of the decision speed $v_1$ on take-off distance and accelerate stop distances

### 3.2.2 Landing Performance

As for the take-off performance calculation, the method analogically applies to the landing performance. Figure 5 shows the landing path definition divided into the approach segment, transition segment and ground roll segment.

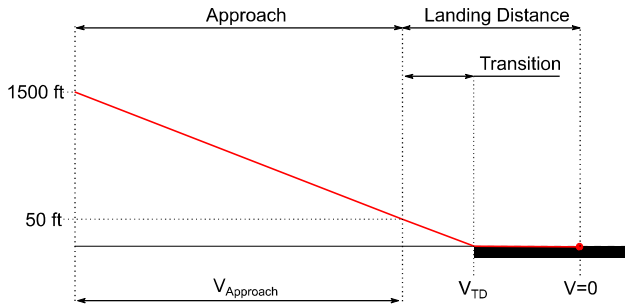


Figure 5 Landing path and definition of various segments [17]

The approach and transition segments start at an altitude of 1500ft and 50ft above airport elevation, respectively, and a constant descent flight path angle of -3° and a constant CAS is assumed. An initial landing mass and speed is prescribed. The aircraft control surfaces are in landing configuration and the landing gear is extended. Once the aircraft touches the ground, the aircraft decelerates by breaking and spoilers are deflected to provide additional drag. The actual landing distance starts at 50ft above airport elevation and continues until the aircraft is completely stopped. For the required landing distance, an additional safety factor of 1/0.6 =1.667 for turbofan engines and a safety factor of 1/0.7 =1.429 for turboprops are required.

### 3.3 Noise Characteristics

This section briefly introduces the methods used in this study for noise evaluation. Worldwide there exist a variety of aircraft noise prediction tools; some are empirical, semi-empirical, analytical or combinations. A comprehensive overview of available programs is given by FILIPPONE [18]. However, there is no tool to this date with a comprehensive interface to the CPACS exchange format. This is partly due to missing exchange data in the CPACS schema definition. The schema extension is currently in development.
While the focus in the development of most aircraft noise prediction methods lies in increasing the accuracy of the applied methods or the breadth of applicability, the current implementation focuses mainly on enabling comparative noise evaluation for various aircraft designs. Precision in noise prediction is therefore not the main objective. Only the most relevant contributors to aircraft noise are addressed and evaluated here, namely the airframe and engine noise.

#### 3.3.1 Airframe Noise

For the airframe noise calculation, semi-empirical formulations on the noise of high-lift devices, wings, control surfaces, and landing gears are used. Therefore, the models by DOBRZYNSKI [19] have been adopted to be evaluated by use of the CPACS data schema and the accompanying TiGL geometry library [20].

#### 3.3.2 Engine Noise

The engine noise evaluation capability is split in turboprop and turbofan engines. For the turbofan engine the exhaust jet and spinning fan are the most dominant contributors to the engine noise. As a comprehensive model with an extensive underlying database for coaxial jet noise, the STONE method [21] is used. The necessary input parameters like exhaust velocity, temperature and cross-sectional jet area can be directly input from the engine *performanceMap* in CPACS. The inlet and outlet noise of the fan on the other hand is evaluated using the KONTOS method [22]. Required inputs for this method, e.g. the fan geometry and characteristics can be found in the engine definition and the *performanceMap* of the CPACS schema.
The noise generated by a propeller is composed of a discrete frequency and a broadband component. The discrete component is due to the rotation of the blades. Two noise sources contribute to this discrete component: the “thickness noise”, which results when a passing blade displaces a volume of air depending on its thickness, and the “loading noise”, which is the acoustic disturbance generated by the local aerodynamic lift forces. Thickness and loading noise are described by a monopole and dipole distribution, respectively. For the calculations in this study, the methods described by GUTIN [23] and DEMING [24] have been adopted. Quadrupole noise induced by non-linear effects is omitted in this study as it occurs only when propeller blades rotate at high speeds [18].
Additionally, effects of atmospheric absorption [25], spreading loss and convective amplification of the sound sources are considered. Ground absorption and noise shielding of fuselage and wing structure is omitted for the sake of simplicity and comparability between different configurations.

## 4 DEMONSTRATION OF RESULTS

The methods for low speed and noise characteristics have been used for the analysis of existing aircraft. The studied aircraft is a DLR internal interpretation of the ATR72 (D070-726) aircraft. Table 1 gives an overview of key aircraft characteristics according to the ATR72 aircraft manual [26] and Figure 6 depict the iso-view of the studies aircraft.

Table 1 Key aircraft characteristics of D070-726 aircraft [26]

| Aircraft | Unit | D070-726 |
|---|---|---|
| Engine Type | [-] | Turboprop |
| No. of Engines | [-] | 2 |
| MTOM | [kg] | 23000 |
| MLM | [kg] | 22350 |
| PAX | [-] | 70 |
| Design Payload | [kg] | 6650 |
| Cruise Mach No. | [-] | 0.439 |
| Design Range | [km] | 1528 |
| Design Cruise Altitude | [-] | 6096 |

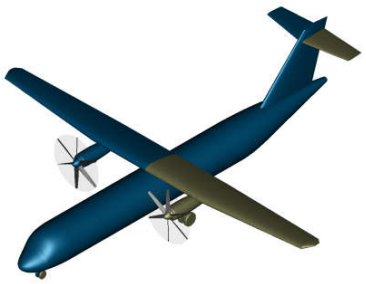

Figure 6 Iso-view of D070-726 aircraft

### 4.1 Take-Off Performance Turboprop

The D070-726 has been analysed with regard to its take-off performance. The low speed performance requirements are listed in Table 2. The requirements are assumed to be the same for the AEO and OEI cases, to have comparability and simplicity of the settings.

Table 2 Take-off performance requirements for the D070-726 test case

| Segment | Parameter | Value |
|---|---|---|
| Ground Roll | Airport elevation<br>Runway slope | 0m<br>0% |
| 2nd | Min. altitude at end | 122m |
| 3rd | Airspeed at end | 170 KCAS |
| Final take-off | Min. altitude at end<br>Flight path angle | 1500ft<br>5° |
| Climb | Thrust lever | 80 % |

Figure 7 shows the altitude and thrust depending on the ground distance for the AEO case, with the same maximum take-off mass. As described in section 3.2.1, each case follows its predefined segments. The AEO case, which corresponds to generic operations, shows a high initial thrust

which reduces due to a decrease in friction drag and thus, less required thrust at the same throttle. During the transition and *2nd segment* as well as the *final segment*, the thrust is nearly constant as the calibrated airspeed is kept constant during the segment and without a significant shift in altitude. At the *3rd segment*, the control surfaces are retracted and drag reduced, thus, less thrust is required for a constant altitude.

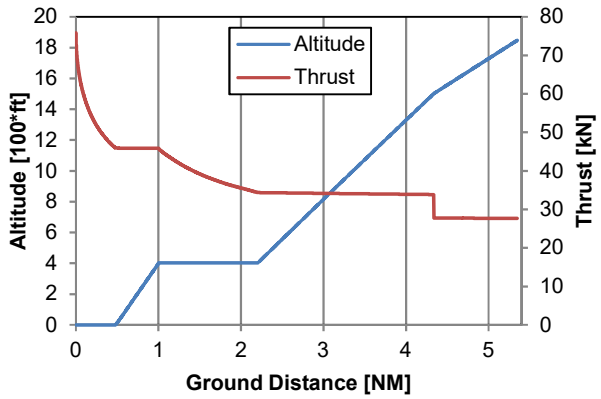


Figure 7 Altitude and thrust over ground distance for AEO take-off cases with 23000 kg TOM at SL, ISA conditions for the D070-726 aircraft.

The balanced field length is analysed by finding the intersection between the OEI and RTO cases during take-off as shown in Figure 8. Prior of analysing the take-off performance results, the D070-726 model has to be calibrated to match the available data of the ATR72 aircraft manual [26]. The calibration is done by specifying a factor for the lift-off speed within the *toolspecific* node of *LSperfo*. Using factors are essential, as they ensure an adjustment for a change in lift coefficient at different airport elevations or take-off masses for subsequent sensitivity studies. After calibration, the results of the D070-726 show a take-off distance of TOD=1335.9m with a decision speed v1=57.11$\frac{m}{s}$ for a MTOM=22.0t. The ATR72 aircraft manual [26] specified a take-off distance of TOD≈1350m with a decision speed v1=57.1$\frac{m}{s}$ for a MTOM=22.0t. Therefore, comparing the ATR manual to the corresponding results show a good agreement with a 1% difference in take-off distance and a matching decision speed.

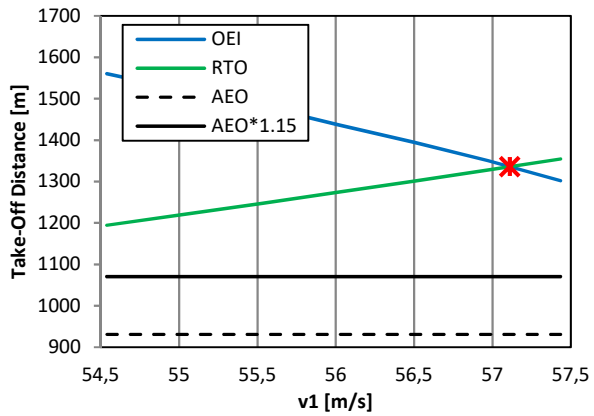


Figure 8 Balanced field length for the D070-726 aircraft with 22000 kg TOM at SL, ISA conditions

To analyse the take-off performance more in detail, different take-off masses and airfield pressure altitudes are computed with the 2nd mode of the performance tool (see Figure 9). Here, the AEO case is used and computes five different take-off masses, ranging from the maximum take-off mass to different payload capacities as well as airfield pressure altitudes up to 3810m. Results show the sensitivity of take-off distance to take-off mass and pressure altitude. As the take-off mass and pressure altitude. increases, the take-off distances increase.

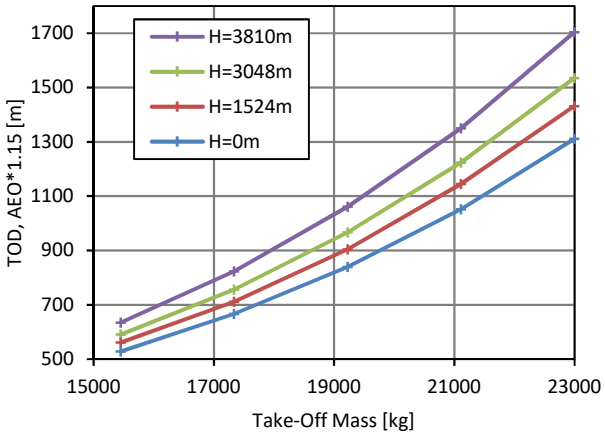


Figure 9 Take-off distances for AEO case at varying airport pressure altitudes and take-off masses at ISA conditions for the D070-726 aircraft.

## 4.2 Landing Performance Turboprop

The approach and landing trajectory for the D070-726 aircraft is depicted in Figure 10. At a flight level of FL15, a constant flight path angle of γ=-3% and a constant CAS is prescribed by the user. The aircraft is in normal landing condition and a flap deflection of 30° with no significant failure of any component. To calibrate the landing performance, factors for the touchdown speed and spoiler drag are specified. The calibrated results by the performance tool show an actual landing distance of ALD=640.1m and a required landing distance of LD=914.45m for an approach speed of $v_{Approch}$=57.1$\frac{m}{s}$ as listed in the ATR72 aircraft manual [26].

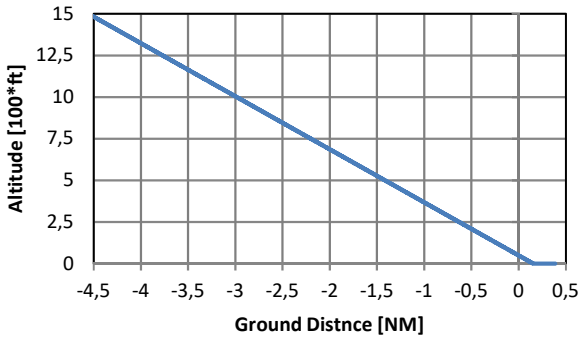


Figure 10 Landing performance of D070-726 at maximum landing mass of 22000 kg at SL, ISA conditions.

Using the calibrated model, a sensitivity study has been performed to study impact of landing mass and pressure altitude on the landing distance (see Figure 11). A linear dependency between an increase in landing distance and an increase in landing mass or pressure altitude is observed.

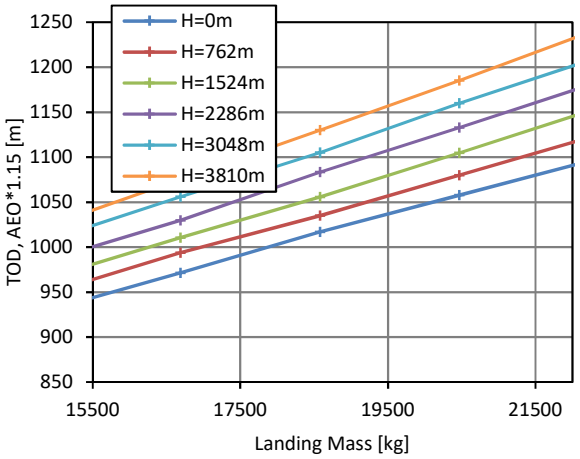


Figure 11 Landing distances for AEO case at varying airport pressure altitudes and landing masses at ISA conditions for the D070-726 aircraft.

### 4.3 Noise Evaluation Turboprop

The noise of the D070-726 configuration has been evaluated subsequent to the low speed performance analysis. The methods described in the preceding section have been used for the estimation of the individual noise sources at the discrete flight points of the take-off and landing trajectory. The overall sound pressure spectra are then calculated at the listener positions according to the noise certification procedure [27]. The resulting noise spectra are weighted in order to result in the effective perceived noise levels (EPNL), measured in the unit EPNdB. These levels can therefore, be compared to measurement values in the database of the EASA [28].

A comparison of the evaluated effective perceived noise levels with the reference values is given in Table 3. As can be seen, the calculated values agree reasonably well with the reference values. Considering the low degree of fidelity of the used method, the accuracy is sufficient for the current study.

Table 3 Comparison of certification noise levels

| | **Sideline [EPNdB]** | **Flyover [EPNdB]** | **Approach [EPNdB]** |
|---|---|---|---|
| ATR72 (EASA) | 82.5 - 82.6 | 76.3 - 80.5 | 92.2 - 92.5 |
| D070-726 | 82.4 | 85.8 | 94.4 |
| Difference | 0.1 | 5.3 | 1.9 |

In order to evaluate the sensitivity of the low-speed take-off and landing performance to the noise evaluation, several trajectories have been calculated with different climb and descent rates, respectively. The take-off and landing trajectories are shown in Figure 12 and Figure 13. The difference between the four take-off trajectories is the prescribed flight path angle in the final take-off segment and altitude of 3rd segment. With regards to the three landing trajectories, the difference is a varying descent angle in the approach segment ranging between the minimum descent angle of 2.1° for L-TR3 and the maximum descent angle of 3.0° for L-TR1.

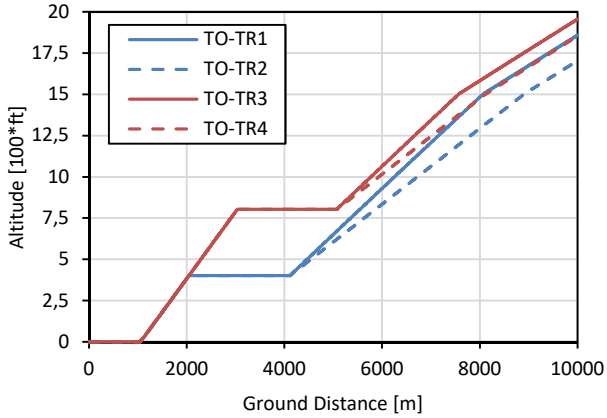


Figure 12 Take-off trajectories for noise assessment.

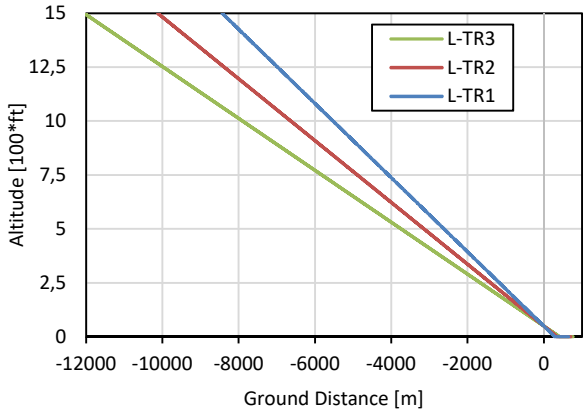


Figure 13 Landing trajectories for noise assessment

The resulting noise levels for the different take-off trajectories are compared in Table 4. For the second flyover trajectory TO-TR2, the EPNL is higher as the aircraft climbs closest to the observer position at 6500m ground distance. The opposite is true for Trajectory TO-TR3, where the aircraft climbs farthest away from the observer and is therefore quieter. Similar trends can be observed for the approach trajectories compared in Table 5 with the trajectory L-TR1 being the quietest and L-TR3 the loudest flight path.

Table 4 Comparison of EPNL for different take-off trajectories

| **Trajectories** | **Flyover [EPNdB]** |
|---|---|
| TO-TR1 | 85.8 |
| TO-TR2 | 86.9 |
| TO-TR3 | 84.3 |
| TO-TR4 | 85.0 |

Table 5 Comparison of EPNL for different landing trajectories

| Trajectories | Approach [EPNdB] |
|---|---|
| L-TR1 | 92.4 |
| L-TR2 | 94.4 |
| L-TR3 | 96.1 |

## 5 CONCLUSION AND OUTLOOK

The presented paper described three methods to extent the DLR tool environment for a conceptual aircraft design process and demonstrated the methods by the D070-726 test case, a turboprop engine aircraft similar to the ATR72.
The new developed engine performance method was an extension of overall aircraft design tool *openAD*. The top-down approach provides an engine deck by assuming an optimised engine at a specific design point and predefined overall gas turbine efficiency. For future work, the engine performance method will be extracted from *openAD* and a standalone tool will be developed to increase the flexibility of the engine design.
The low speed performance tool comprises the take-off and landing path computation by solving the 2D equation of motion with a constant time step. Different operating conditions are evaluated i.e. all engine operating (AEO), one engine inoperative (OEI) and rejected take-off (RTO). The tool can be used within the L1 level of the aircraft design process (see Figure 1) using the AEO operating condition but also, in the subsequent post-processing segment for a more detailed analysis. The take-off and landing performance results of the D070-726 configuration test case are in good agreement with the provided data by the manufacturer.
Finally, the noise characteristics are estimated by its most relevant contributors, namely the airframe and engine noise. The airframe noise uses a semi-empirical formulation and considers high-lift devices, wings, control surfaces, and landing gears. The engine noise estimation is split in turboprop and turbofan engines. By comparing the D070-726 test case to the measured values of EASA, the calculated certification noise levels show a reasonable agreement. Further studies are planned to evaluate turbofan engine aircraft and different aircraft classes.

## REFERENCES


[1] EUROPEAN COMMISSION , „Flightpath 2050 Europe's Vision for Aviation," European Union, Belgium, 2011.

[2] D. Seider, P. M. Fischer, M. Litz, A. Schreiber und A. Gerndt, „Open Source Software Framework for Applications in Aeronautics and Space," IEEE Aerospace Conference, Montana, USA, 2012.

[3] M. Alder, E. Moerland, J. Jepsen und N. Björn, „Recent Advances in Establishing a Ccommon Language for Aircraft Design with CPACS," Aerospace Europe Conference 2020, Bordeaux, France, 2020.

[4] C. M. Liersch und M. Hepperle, „A Distributed Toolbox for Multidisciplinary Preliminary Aircraft Design," CEAS Aeronautical Journal, Bermen, Germany, 2011.

[5] S. Wöhler, G. Atanasov, D. Silberhorn, B. Fröhler und T. Zill, „Preliminary Aircraft Design within a Multidiciplinary and Multifidelity Design Environment," Aerospace Europe Conference 2020, Bordeaux, France, 2020.

[6] S. Reitenbach, M. Vieweg, R. Becker, C. Hollmann, F. Wolters, J. Schmeink, T. Otten und M. Siggel, „Collaborative Aircraft Engine Preliminary Design using a Virtual Engine Platform, Part A: Architecture and Methodology," AIAA SciTech Forum 2020, Orlando, USA, 2020.

[7] L. Bertsch, „Noise Prediction within Conceptual Aircraft Design," DLR Forschungsbericht, ISRN DLR-FB–2013-20, 2013.

[8] L. Bertsch, I. A. Clark, R. H. Thomas, L. Sanders und I. LeGriffon, „The Aircraft Noise Simulation Working Group (ANSWr) - Tool Benchmark and Reference Aircraft Results," 25th AIAA/CEAS Aeroacoustics Conference, Delft, The Netherlands, 2019.

[9] E. Torenbeek, Synthesis of Subsonic Airplane Design, Netherlands: Springer Netherlands, 1982.

[10] E. Torenbeek, „Advanced Aircraft Design," Wiley Aerospace Serices, Delft, Netherlands, 2013.

[11] J. Roskam, Airplane Design Part 1-7, DARcorporation, 1985 - 1990.

[12] D. Raymar, Aircraft Design: A Conceptual Approach, AIAA Education Series, 1989.

[13] D. P. Wells, B. L. Horvath und L. A. McCullers, „The Flight Optimization System -Weights Estimation Methods," NASA Langley Research Center, Virginia, USA, 2017.

[14] L. R. Jenkinson, P. Simpkin und D. Rhodes, „Civil Jet Aircraft Design," Butterworth Heinemann, United Kingdome, 1999.

[15] D. Silberhorn, „AMC – Aircraft Mission Calculator; Documentation," German Aerospace Center,, Hamburg, Germany, 2020.

[16] W. J. Brauenling, Flugzeugtriebwerke, 4. Hrsg., Hamburg: Springer Vieweg, 2015.

[17] Customer Service, „getting to grips with aircraft performance," Airbus, France, 2002.

[18] A. Filippone, „Aircraft Noise Prediction," *Progress in Aerospace Sciences,* Nr. 68, pp. 27-63, 2014.

[19] W. Dobrzynski, „Konfigurationen 2020 Abschlussbericht-Konfigurative Lärmkriterien, final project report, ref.-nr. K2020-DLR-000-017-P4-Final Report," Braunschweig, 2007.

[20] M. Siggel, J. Kleinert, T. Stollenwerk und R. Maierl, „TiGL: An Open Source Computational Geometry Library for Parametric Aircraft Design," *Mathematics*

*in Computer Science,* Bd. 13, Nr. 3, pp. 367-389, 2019.

[21] J. R. Stone, D. E. Groesbeck und C. L. Zola, „Conventional Profile Coaxial Jet Noise Prediction," *AIAA Journal,* Bd. 21, Nr. 3, pp. 336-342, 1983.

[22] K. B. Kontos, B. A. Janardan und P. Gliebe, „Improved NASA-ANOPP noise prediction computer code for advanced subsonic propulsion systems," Cincinnati, 1996.

[23] D. B. Hanson, „Near-Field Frequency-Domain Theory for Propeller Noise," *AIAA Journal,* Bd. 23, Nr. 4, pp. 499-504, 1985.

[24] N. Peake und W. K. Boyd, „Approximate method for the prediction of propeller noise near-field effects.," *Journal of aircraft,* Bd. 30, Nr. 5, pp. 603-610, 1993.

[25] „ISO 9613-1, Acoustics—attenuation of sound during propagation outdoors—part 1: calculation of the absorption of sound by the atmosphere.," International Organization for Standardization, 1993.

[26] A. 72, Flight Crew Operating Manual, 1999.

[27] International Civil Aviation Organization, „Environmental Technical Manual-Volume I: Procedures for the Noise Certification of Aircraft".

[28] European Union Aviation Safety Agency, [Online]. Available: https://www.easa.europa.eu/domains/environment/easa-certification-noise-levels. [Zugriff am 20 08 2020].

[29] M. Koch und L. Bertsch, „Engine noise source placement for shielding calculation," in *Inter-Noise 2019*, Madrid, 2019.

[30] J. Roskam, Airplane Design Part I to VII, DARcorporation, 1985 - 1990.

[31] Avions de Transport Régional, „CM Marketing," 2017.

[32] International Organization for Standardization, „ISO 9613-1, Acoustics—attenuation of sound during propagation outdoors—part 1: calculation of the absorption of sound by the atmosphere.," 1993.